

Journal of Materials Chemistry B

Accepted Manuscript



This is an *Accepted Manuscript*, which has been through the Royal Society of Chemistry peer review process and has been accepted for publication.

Accepted Manuscripts are published online shortly after acceptance, before technical editing, formatting and proof reading. Using this free service, authors can make their results available to the community, in citable form, before we publish the edited article. We will replace this *Accepted Manuscript* with the edited and formatted *Advance Article* as soon as it is available.

You can find more information about *Accepted Manuscripts* in the [Information for Authors](#).

Please note that technical editing may introduce minor changes to the text and/or graphics, which may alter content. The journal's standard [Terms & Conditions](#) and the [Ethical guidelines](#) still apply. In no event shall the Royal Society of Chemistry be held responsible for any errors or omissions in this *Accepted Manuscript* or any consequences arising from the use of any information it contains.

ARTICLE

Supermolecular Theranostic Capsules for pH-Sensitive Magnetic Resonance Imaging and Multi-responsive Drug Delivery

Di-Wei Zheng^a, Qi Lei^b, Si Chen^b, Wen-Xiu Qiu^b, Meng-Yi Liu^a, Xian Chen^a, Yu-Xue Ding^a, Peng-Hui Li^c, Quan-Yuan Zhang^a, Zu-Shun Xu^a, *, Xian-Zheng Zhang^b, **, Paul K. Chu^{c,***}

Received 00th January 2015,
Accepted 00th January 2015

DOI: 10.1039/x0xx00000x

www.rsc.org/

Magnetite (Fe₃O₄) microcapsules prepared by layer-by-layer self-assembly are investigated as multi-functional magnetic resonance imaging contrast agents and drug carriers. They are produced by the host-guest interaction and Coulombic force from different supramolecular polymers. Drug molecules are released controllably from the microcapsules by non-invasive ultra-violet light induced photo-isomerization of the azobenzene molecule and pH sensitive Schiff's base. In addition, by encapsulation of the superparamagnetic iron oxide nanoparticles (SPION) in the nearby layers, magnetic field targeting and MRI contrast are achieved. Under tumor-like acidic conditions (pH = 5.6), the r₂ relaxivity of the microcapsules is 126 mM⁻¹S⁻¹ which is 37% larger than that in neutral environment (92 mM⁻¹S⁻¹). As a result of the low pH enhanced MRI contrast agent, the tumor structure can be observed clearly *in vivo* confirming the high efficacy as a negative MRI agent in T₂-weighted imaging. The materials as combined carriers have great potential in clinical applications in drug delivery and contrast agents in MRI.

Introduction

Cancer is one of the most serious public health problems worldwide. According to the World Health Organization (WHO), more than 15 million people will suffer from cancer in 2020 and two thirds of them will die each year¹. Since most of the early-stage cancer can be treated effectively, it is essential to develop *in vivo* imaging technology to determine tumor locations. Magnetic resonance imaging (MRI) is an effective way to image tumors based on different proton density and/or relaxation time. Superparamagnetic iron oxide nanoparticles (SPION) are cheaper and non-toxic, and are widely used in T₂ MRI². T₂ relaxation is affected by the microenvironment around the nanoparticles and so the materials can be used as pH response MRI nanoprobes to detect specific lesions in both functional and morphological imaging³. With the development of imaging technologies such as MRI, CT, and PET, the combination of two or more imaging modalities can get more information about diseases. Hence, multiple imaging systems based on SPION such as MRI-fluorescence⁴, MRI-photoacoustics⁵, and MRI-CT⁶ have been developed. Furthermore, materials that serve as both MRI contrast agents and drug delivery systems can achieve functions of diagnosis and treatment at the same time⁷.

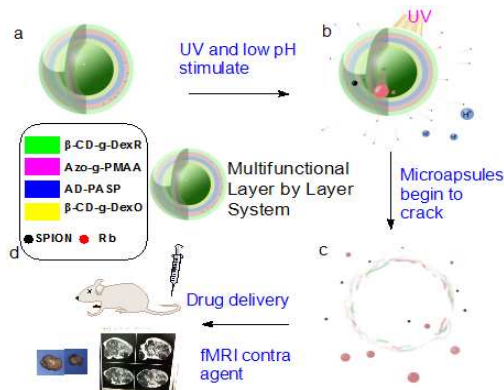
Chemotherapy, one of the most effective methods to treat cancer besides radiotherapy and surgical treatment, still suffers from serious side effects which limit further clinical application. To deliver a high dose of drug to specific tumors and reduce side effects, drug delivery systems (DDS) such as polymer micelles⁸, vesicles⁹, nanospheres¹⁰, hydrogels¹¹, and mesoporous nanoparticles¹² have been proposed. Because of low pH (pH < 6.8), high temperature (T > 37 °C), and reducing microenvironments in the tumor sites, many drug delivery systems with passive target have been introduced. For instance, Paul Ehrlich's¹³ concept of a "magic bullet"¹⁴⁻¹⁸, and a combined system possessing stimulates-respond drug delivery and SPION based MRI capabilities has been reported¹⁹.

Macromolecular drugs based on peptides and proteins such as Avastin, neocarzinostatin, and tumor necrosis factors have attracted much attention as anti-cancer drugs²⁰⁻²² and it is important to develop drug delivery systems with the ability to transport macromolecular drugs. Recently, dual stimuli-responsive composites such as light and temperature responsive materials, matrix metalloproteinase, and pH-sensitive system have been reported^{23,24}, but there have been few investigations on tri-sensitive (pH, magnetic, and photosensitive) composites

1 | J. Mater. Chem. B, 2015, 00, 1-3

that possess both drug delivery and stimulant-responsive imaging functions.

In this article, a new kind of supramolecular polymer was synthesized. PAH(Azo-g-PMAA/ β -CD-g-DexR)₅/PAH/AD-PASP/(β -CD-g-DexO/AD-PASP)₃/PAH/SPION/PAH/((AD-PASP/ β -CD-g-Dex(O))₂) multilayered microcapsules was prepared (Scheme 1). Although light is an accurate medium to trigger targeted drug delivery^{25,26}, prolonged ultraviolet (UV) exposure harms cells and lacks tissue penetration ability in this respect, the dual responsive system described herein offers a solution. In this system, a magnetic field is used to aggregate microcapsules to a specific area and then a UV light beam is directed specifically to the microcapsules to release the drug. Herein, the host-guest interaction between Azo-g-PMAA and β -CD-g-DexR is weakened by UV exposure with the photoisomerization of azobenzene²⁷. Because β -CD is grafted with PAD through low pH-sensitive Schiff's bond, the β -CD of CD-g-DexO and AD-PASP connected to it can break down from PAD in an acidic tumor environment, leading to the disassembly of the capsules and the release of drugs. Thus, the drug release can be controlled accurately. In this way, the effectiveness of chemotherapy can be improved while undesirable side effects can be avoided. Owing to the magnetic targeting ability of SPION, the microcapsules can be concentrated to a certain location *in vivo* thus producing precise targeting and controlled release. Furthermore, by taking advantage of the T2 imaging ability of SPION, the LBL microcapsules can be utilized to diagnose tumor positions *in vivo*. Our results show that protonation of carboxyl groups in an acidic environment leads to slower water exchange and increases the relaxation rate by 37%. The microcapsules are especially useful in a low pH micro-environment typical of cancer as well as MRI theranostic systems.



Scheme 1. Schematic illustration of the multi-responsive polymer/Fe₃O₄ complex theranostic capsule in MR imaging and drug delivery: (a) Preparation of the microcapsules with theranostic functions; (b) Using 365 nm ultraviolet light and acidic conditions to control the release characteristics of the microcapsules; (c) Under the stimulation, the microcapsules crack and the model drug is released; (d) After subcutaneous injection, the tumor is observed clearly by MRI.

Experimental section

Materials and methods

Poly (allylamine hydrochloride) (PAH, MW~15,000), Fetal Bovine Serum (FBS) and fluorescein isothiocyanate (FITC) were purchased

from Sigma Aldrich. Amantadine hydrochloride (AD) and poly (styrenesulfonic acid sodium salt) (PSS, MW ~ 70,000) were purchased from J&K Chemical Ltd. Calcium chloride (CaCl₂), potassium carbonate (K₂CO₃), β -cyclodextrin (β -CD), p-methyl benzene sulfonic chloride (p-TsCl), acetone, methanol, trimethylamine (TEA), dimethyl formamide (DMF), phosphoric acid (H₃PO₄), L-aspartic acid, sodium hydroxide (NaOH), hydrochloric acid (HCl), and ammonium hydroxide were purchased from Shanghai Reagent Chemical Co. (PR China). Rhodamine B, dextran (MW ~ 70,000), methacrylic acid (MAA), sodium borohydride (NaBH₄), p-aminoazobenzene, acryloyl chloride, azodiisobutyronitrile (AIBN), ferric trichloride hexahydrate (FeCl₃·6H₂O), ferrous chloride tetrahydrate (FeCl₂·4H₂O), periodate potassium (KIO₄), ethanediamine (EDA), and ethylene diamine tetraacetic acid (EDTA) were purchased from Aladdin Industrial Corporation. The synthesis process is illustrated in Scheme 2.

Synthesis of Ethanediamine- β -CD (EDA- β -CD)

EDA- β -CD was synthesized by the reaction between mono-6-(p-tolylsulfonyl)- β -cyclodextrin (OTs- β -CD) and EDA. 10 g of β -CD were added in 300 mL of 0.4 M NaOH solution under stirring and then 15 g of p-TsCl were added slowly (1 g/min) in an ice bath. After vigorous agitation for about 1 h at room temperature, the suspension was filtered and hydrochloric acid was added until the pH value reached to 6. After cooling to 4 °C overnight, the precipitate was filtrated and rinsed with acetone three times. The crude product was recrystallized at 60 °C in water for three times. After drying at 50 °C for 48 h under vacuum, the OTs- β -CD powder was obtained. 5.0 g of the OTs- β -CD were put in 30 mL of anhydrous EDA and the reaction proceeded at 80 °C for 48 h. Afterwards, the solution was cooled to room temperature and poured into a large amount of ethanol. The precipitate was collected and dissolved in water/methanol (3:1 v/v). After repeating twice of the precipitation and dissolution procedures, the final product was dried at 50 °C for 48 h under vacuum and the white EDA- β -CD powder was collected.

Synthesis of Dextran-graft- β -CD (β -CD-g-Dex)

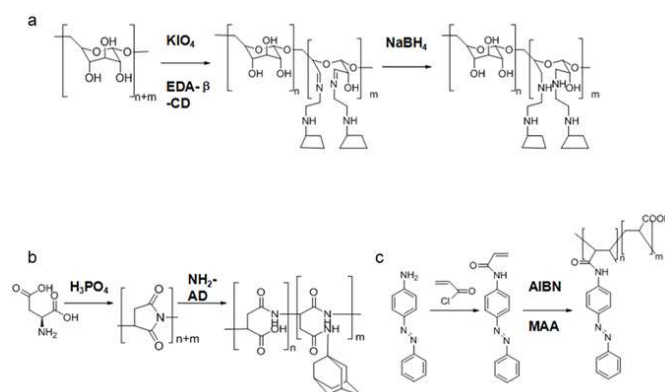
1.00 g of dextran was dissolved in 40 mL of DI water and the solution was purged with N₂ for 30 min. 0.142 g of KIO₄ were then added and the mixture was stirred at 25 °C for 12 h under N₂. The solution was poured into methanol and the white precipitate polyaldehyde dextran (PAD) was collected, followed by vacuum drying for 24 h. 0.50 g PAD was dissolved in 30 mL of DI water and the solution was purged with N₂ for 30 min. Afterwards, 20 mL of the EDA- β -CD solution was added and the mixture was stirred at 30 °C for 24 h under N₂. After formation of the Schiff's base, β -CD was grafted to dextran with the pH-sensitive chemical bonds, and the solution became from colorless transparent to yellow. The solution was dialyzed (MWCO: 14000 Da) against DI water for 5 days and lyophilized for 3 days to obtain the yellow β -CD-g-Dex solid.

Reduction reaction of Schiff's base

40 mL of an aqueous β -CD-g-Dex (0.5 g) solution and 1.9 g of NaBH₄ were added and the mixture was reacted for 48 h at room temperature under stirring. The solution was dialyzed (MWCO: 14000 Da) against DI water for 6 days and lyophilized for 3 days to obtain β -CD-g-Dex without C=N bonds. The yellow solution turned colorless gradually during the process.

Synthesis of Poly(aspartic-graft-adamantane) (AD-g-PASP)

AD-g-PASP was synthesized according to the literature²⁸. Briefly, 15.0 g of L-aspartic acid and 7.5 g of H₃PO₄ were charged in a 250 mL round-bottomed flask which was placed in a rotary evaporator and the reactor was heated to 180 °C under reduced pressure and maintained at this temperature for 2.5 h. The crude product was dissolved in 100 mL of DMF. The solution was added to water dropwise (1 drop in five seconds) to form a white precipitate. The white precipitate was collected and rinsed twice with DI water. After drying in a vacuum oven at 110 °C for 24 h, a product of PSI was obtained. A solution of AD-HCl (0.30 g, 1.55 mmol, 15% of the PSI repeat unit) in DMF (10 mL) was added to a solution of PSI (1.0 g, 10.3 mmol repeat unit) in DMF (15 mL). The mixture was purged with N₂ under stirring at 70 °C for 24 h and then cooled to room temperature. An aqueous NaOH (0.38 g of NaOH in 20 mL of DI water) was dropwise added at a rate of about 1 drop per 20 seconds with an ice bath. The suspension was stirred overnight at room temperature. Then a solution of HCl was added to adjust the pH value to 7.0 and dialyzed (MWCO: 14000 Da) against DI water for 3 days. Afterwards, the solution was lyophilized for 3 days to obtain the white AD-g-PASP solid.



Scheme 2. Synthetic procedure: (a) β -CD-g-Dex, (b) AD-g-PASP, and (c) Azo-g-PMAA.

Synthesis of azobenzene graft polymethylacrylic acid (Azo-g-PMAA)

4-phenylazophenylacrylamide was synthesized according to the literature²⁹. 1.61 g of 4-aminoazobenzene and 1.46 mL of triethylamine were dissolved in 40 mL of tetrahydrofuran. 0.8 mL of acryloyl chloride were dissolved in 15 mL of tetrahydrofuran and added dropwisely with stirring at 0 °C under a nitrogen atmosphere. The mixture was filtered and washed with water 3 times to remove triethylammonium chloride and the product was obtained after solvent evaporation and vacuum drying.

0.77 g of MMA and 0.56 g of 4-phenylazophenylacrylamide were dissolved in 7.5 mL of DMF together with 100 mg of AIBN as an initiator. The solution was purged with N₂ and stirred at 65 °C for 24 h. After the reaction, the crude product was precipitated with water. A sodium hydroxide solution was used to wash the precipitate. Azo-g-PMAA was then dissolved in the sodium hydroxide solution and HCl was used to adjust the pH value to 8–9, then the mixture was dialyzed (MWCO: 3500 Da) against water at a pH of 8 for 6 days. The sample was lyophilized for 3 days to obtain the orange Azo-g-PMAA powder.

Preparation of iron oxide nanoparticles

SPION was prepared according to the literature procedure³⁰. 13.10 g of FeCl₃·6H₂O and 6.65 g of FeCl₂·4H₂O were mixed in 80 mL of DI water. The solution was stirred under nitrogen for 0.5 h and 45 mL of NH₃·H₂O were added dropwise at 80 °C. 7.5 g of citric acid in 15 mL of water were introduced after the temperature rose to 95 °C and stirred for 90 min. The solution was dialyzed against water with a dialysis bag (MWCO: 14000 Da) to obtain a stable magneto fluid.

Preparation of fluorescein loaded calcium carbonate

A solution of dextran (0.5 g) in DMSO (30 mL) and 15 mg of FITC were charged into a 50 mL round bottom flask, and the mixture was stirred for 24 h at room temperature. The solution was dialyzed against water in a dialysis bag (MWCO: 14000 Da) and freeze-dried to obtain the yellow powder. 0.228 g of K₂CO₃ and 10 mg of PSS were dissolved in 5 mL of water and 0.183 g of CaCl₂ and 5 mg of FITC-dextran were dissolved in 5 mL of water. The CaCl₂ solution was poured into the K₂CO₃ solution under vigorous stirring for 30 s and stood for two minutes. The calcium carbonate microspheres were collected by filtration.

Fabrication of LBL microcapsules

CaCO₃ particles were used as the colloid template in the fabrication of microcapsules. 100 mg of the CaCO₃ microspheres were dispersed in 1 mL of PAH polycation solution (1 g/L) and the suspension was agitated for 15 min to produce the PAH layer. After adsorption, the particles were isolated by centrifugation (4,000 rpm for 1 min) and rinsed with 2 mL of DI water twice. LBL assembly of the other polymers on the CaCO₃ particles was repeated using the same method. The LBL process was repeated to produce the (PAH(Azo-g-PMAA/ β -CD-g-DexR)₅/PAH/AD-PASP/(β -CD-g-Dex O/AD-PASP)₃/PAH/SPION/PAH/(AD-PASP/ β -CD-g-Dex (O)₂) microcapsules. 0.4 M of the EDTA solution with pH of 7.4 were added to remove the CaCO₃ core and the capsules were collected under a magnetic field and rinsed with DI water twice.

Characterization

¹H NMR was used to determine the chemical structure of Azo-g-PMAA, β -CD-g-Dex(O), β -CD-g-Dex(R), and AD-PASP. It was conducted on the UNITY INVOA 600 MHz spectrometer (Varian, USA) with DMSO-d₆ and D₂O-d₂ as the solvents. The morphology of the hollow microcapsules, calcium carbonate microspheres, and SPION were examined by transmission electron microscopy (TEM, Tecnai G20, FEI Corp., USA) and scanning electron microscopy (SEM FEI-QUANTA 200). Prior to conducting TEM, a drop of the concentrated capsule solution was deposited on a copper grid and dried in air and before performing SEM, a drop of the concentrated capsule solution was dried and coated with gold for 150 s. The iron content in the microcapsules was determined by atomic absorption (Varian SpectrAA-240FS). The microcapsule powders (50 mg) was added to a conical flask, completely digested in a solution of nitric acid (3.5 g) at 75 °C, and dried by heating. Afterwards, DI water (50 mL) was added to dissolve the ferric salt and transferred to a centrifuge tube. The iron content in the solution was determined at the specific Fe absorption wavelength of 248.3 nm. Fourier transform infrared spectroscopy (FTIR) was carried out on the Transform Infrared spectrometer (Perkin Elmer Spectrum USA). The amount of drug released from the capsules was determined on the Fluorescence spectrophotometer (Perkin Elmer Spectrum). The cells after co-

incubation were viewed by confocal laser scanning microscopy (CLSM, Nikon C1-si, Japan) and the magnetic properties were assessed on a vibrating sample magnetometer (VSM, HH-15, China) at 298 K under an applied magnetic field.

In vitro drug release at different environment

The microcapsules were divided into four groups with 30 mg of microcapsules in each group. The release experiments was carried out using a dialysis method. Briefly, 30 mg of the microcapsules were dispersed in 1 mL of DI water, charged into a dialysis tube (MWCO: 14,000 Da), and immersed in 250 mL of the buffer solutions (PBS for pH 7.4 and acetate for pH 5.6, 50 mM) under stirring at 37 °C. At a specific time point, 4 mL of the dialysis medium was taken out for fluorescence analysis and replenished with the same volume of fresh media. Dextran release into the buffer was assessed by 365 nm UV light using a similar procedure. The amount of the dextran released to the dialysis medium was measured on a fluorescence spectrometer and all the measurements were performed in triplicates in darkness. Since the fluorescent response of FITC may be affected by other materials in the solution. UV-vis Spectrophotometer is also used to

well was discarded, then the PBS solution (100 mL/well) was added to wash the cells. 200 mL of the microcapsules solutions with different concentrations (dose diluted by the DMEM culture medium, 0-0.1 mg/mL) were added to each well to culture the HeLa cells at 37 °C for 24 h. The medium was discarded and 100 mL PBS was added to each well to wash the cells. The MTT solution (100 mL, 0.5 mg/mL) in the serum free DMEM medium was added to each well and incubated with the HeLa cells at 37 °C for another 4 h. Afterwards, the medium was discarded and DMSO (100 mL/well) was added to dissolve the precipitate. Light absorption was monitored at 570 nm on a microplate reader. The relative cell viability was determined by the following equation: Relative cell viability (%) = $(OD_{\text{treated}} - OD_{\text{background}}) / (OD_{\text{control}} - OD_{\text{background}}) \times 100$, where OD_{treated} was obtained from the cells treated with the microcapsules, OD_{control} from the untreated control cells, and $OD_{\text{background}}$ from the empty well.

Co-Incubation of microcapsules with Cells at Different pH Values

HeLa cells were incubated in the DMEM medium with 10% FBS and 1% antibiotics (penicillin-streptomycin, 10,000 U/mL) at 37 °C in a humidified atmosphere containing 5% CO₂. The cells were seeded on a 96 well plate at a density of 1×10^5 cells/well and incubated in 1 mL of DMEM containing 10% FBS for 24 h. Afterwards, the microcapsules were dispersed in 2 mL of the DMEM medium with 10% FBS and 1% antibiotics. For the group with UV irradiation, cells was exposed to UV for 10 min (ZF-7A, China, 8 W). After co-incubation for 4 h at 37 °C, the medium was removed and the cells were washed with 1 mL of PBS, then observed by CLSM.

In vitro relaxivity measurement

To determine the relaxivity of microcapsules, the suspensions containing the microcapsules were diluted with distilled water and mixed with a 1% (w/v) agar solution to obtain a final iron concentration in the range of 0.0625-1 mmol/L. The samples were transferred to a NMR tube and the T₂ relaxation time was determined on a clinical 9.4T MR scanner. The T₂ relaxation rates (1/T₂) were plotted against the iron concentrations and the T₂ relaxivity was calculated by a linear fit. 1/T₂-[Fe] curves was shown in Figure S2.

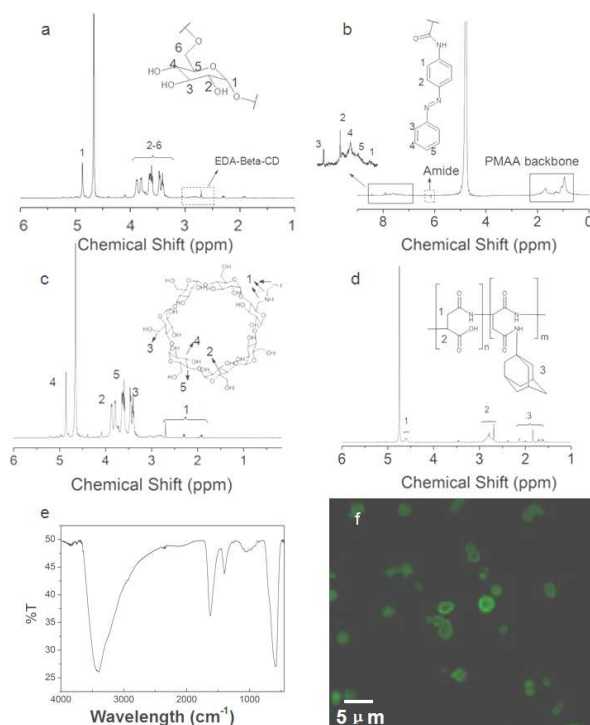
In vivo MRI and in vivo magnetic targeting experiment

The *in vivo* MR imaging experiments were performed on KM mice (weight of 25 g). The procedures were in accordance with the protocols of the Institutional Animal Care and Use Committee at Hubei University and also approved by the Institutional Animal Care. The mice were scanned before and after subcutaneous injection of the microcapsules solution at a dose of 12.5 mg Fe/kg body weight. The T₂-weighted coronal MR images were acquired on the MR scanner before and at 0.5 h, 1h and 2h post injection.

The mice were subcutaneous injected with the microcapsules solution at a dose of 12.5 mg Fe/kg body weight. Magnets were placed above the tumors. After magnetic targeting for 48 h, the mice were sacrificed and tumors were collected for HE staining and Prussian blue staining.

In vivo acute toxicity test

In order to study the acute toxicity, the LD₅₀ of the microcapsules was investigated. For the acute toxicity test, the first mouse received a dose one step below the assumed estimate of the LD₅₀ of 100 mg/kg.



study the drug release behavior of the microcapsules (Absorption peak at 488 nm).

Figure 1. ¹H-NMR spectra of (a) β-CD-g-Dex(O), (b) Azo-g-PMAA, (c) EDA-β-CD, and (d) AD-g-PASP; (e) UV-vis spectrum of β-CD-g-Dex; (f) CLSM image of the micro-capsule.

In vitro cytotoxicity test

The *in vitro* toxicity of the microcapsules was determined by standard MTT assay with HeLa cells. The HeLa cells were seeded on 96-well plates at a density of $1-1.2 \times 10^4$ viable cells per well, then cultured for 24 h at 37 °C and 5% CO₂. The DMEM medium in each

If the animal survives, the second animal receives a higher dose. If the first animal dies, the second animal receives a lower dose. If the LD₅₀ of the microcapsules is up to 1000 mg/kg, which was far more than the require does, the microcapsules should be non-toxic *in vivo*.

Histochemistry and Optical Imaging

Tissue samples were fixed with paraformaldehyde 12 h after administration of the solution of FMCNPs (dosage of 12.5 mg Fe/kg body weight). The tumor slices from the control group (without injection of FMCNPs) were obtained in the same way. Prior to the chemical analysis, tissue samples were processed with Prussian blue staining or hematein eosin staining.

In vitro Stability Test

1 mg/ml of the microcapsules was added into 5 mL of PBS, DMEM containing 10% FBS and BSA (2 mg/mL), respectively. 12 h after, the microcapsules was observed by using CLSM. For the protein adsorption assay, 1 mL of microcapsules solution (1 mg/mL) was added to 1 mL BSA solution. The concentration of BSA in the supernatant was determined from its characteristic UV absorbance (280 nm) (2 mg/mL). After shaking at 37 °C for 0.5 h and following centrifugation, the upper layer was carefully collected. The concentration of BSA in the supernatant was determined from its characteristic UV absorbance (280 nm), using a calibration curve obtained from BSA solutions of known concentrations. The protein adsorbed on the microcapsules was calculated using following equation:

$$q = \frac{(C_i - C_s) / V}{m}$$

where C_i and C_s are the initial BSA concentration and the BSA concentration in the supernatant after adsorption experiments, respectively; V is the total volume of the solution (2 mL); and m is the weight of the microcapsules (1 mg) added into the solution.

Results and discussion

Characterization of Dex-g-β-CD and PMAA-g-Azo

Four kinds of biocompatible polymers, β-CD-graft-dextran (β-CD-g-Dex), adamantane-graft-poly (aspartic) (AD-g-PASP), azobenzene-graft-polymethylacrylic acid (Azo-g-PMAA), and β-CD-graft-dextran (reduced form) (β-CD-g-Dex R) were synthesized and used in this article. β-CD-g-Dex was synthesized by forming the Schiff's base between polyaldehyde dextran (PAD) and mono-6-deoxy-6-ethanediamine-β-CD (EDA-β-CD), after reduction, pH sensitive C=N bonds were formed which can be used to assemble with polyaspartic acid-graft-adamantane (AD-g-PASP). β-CD and the guest molecule linkers are broken down from PAD in an acidic environment and the azobenzene molecules are grafted to polymethylacrylic acid. The configuration of azobenzene is switched with 365 nm UV light exposure.

The ¹H NMR spectrum of β-CD-g-Dex was shown in Fig. 1a. The peaks at δ 2.6 and δ 3.1 are attributed to protons at positions 4 and 1 in EDA-β-CD and that at δ 4.8 is due to protons at position 1 contributing to an anomeric carbon atom. There is no peaks appeared between δ 5.0 and 5.7 indicating that the aldehyde groups of PAD are fully replaced by EDA-β-CD. The three characteristic peaks between δ 4.0 and 3.2 were linked to protons at positions C₂-C₆ of dextran³¹. As shown in Fig. 1b, the peaks around δ 1 were attributed to the protons of methyl groups in PMAA and those around δ 2 are due to

the alkyl chain of PMAA. Weak peaks appeared at δ 7.0~ 8.0 were associated with azobenzene. Fig. 1c showed the ¹H NMR spectrum of EDA-β-CD. Peaks at δ 2 to δ 3 was due to the alkyl chain in ethanediamine. In the ¹H NMR spectrum of AD-g-PASP (Fig. 1d), the peaks at around δ 2 were due to the protons of adamantane. According to the UV-Vis spectrum of β-CD-g-Dex, the peak at 334 nm disappears after the reduction reaction, indicating that C=N bonds are fully converted to C-N bonds.

Synthesis of Fe₃O₄ nanoparticles

Citric acid is used to decorate the naked SPION. As shown in the FT-IR spectrum (Fig. 1f), the broad peak near 3,400 cm⁻¹ and the zeta potential was -18.8 mV showed that the surface of SPION was successfully modified by carboxyl groups. This result confirmed that citric acid was modified on the surface of SPION. TEM micrograph was shown in Fig. 2b, regular SPION with a diameter of about 10 nm could be observed.

Composition and morphology of microcapsules

The morphology of the microcapsules was examined by TEM. The CLSM image of microcapsules was shown in Fig. 1f, green fluorescence was due to the FITC-dextran core. As shown in Fig. 2c and d, after the removing of CaCO₃, the wall of the microcapsules collapsed and Fe₃O₄ nanoparticles were distributed equally in the wall. The zeta potential of the microcapsules was -34.5 mV, mainly because of the accumulation of PASP and PMAA polyanions.

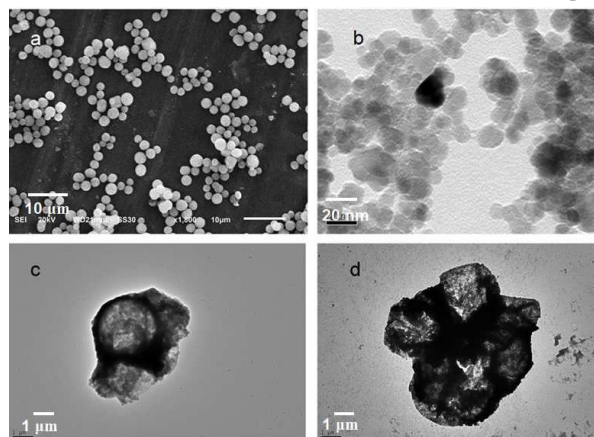


Figure 2. (a) SEM image of calcium carbonate microspheres; (b) TEM image of SPION; (c) and (d) TEM images of the microcapsules.

Iron content and magnetic targeted test of microcapsules

The iron content determined at the Fe absorption wavelength of 248.3 nm by ICP-AES was 7.41 mg/L and the mass of iron in the microcapsules was about 0.57%. Even through only one layer of Fe₃O₄ nanoparticles was introduced, the microcapsules was concentrated to a specific area with magnetite (Figs. 3a and 3b). In fact, this favorable characteristic enabled fast and accurate non-invasive tumor targeting. As shown in Fig. 3c, the vibrating sample magnetometer (VSM) test performed at room temperature reveals the typical form of magnetization versus applied magnetic field. A large magnetic moment in the presence of an external magnetic field B₀ was observed but there was no remnant magnetic moment when the field is zero, thus indicating a superparamagnetism feature. Even through the iron particles were trapped in the microcapsules, the saturation magnetization values was still as high as 18.94 emu.

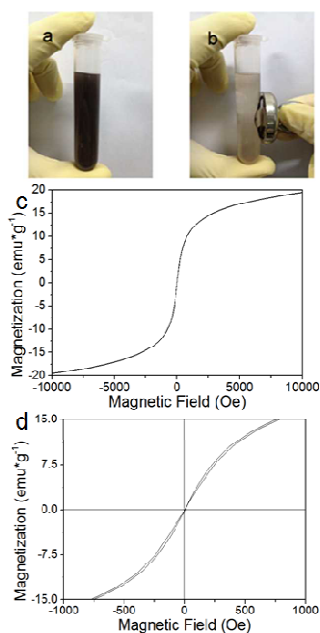


Figure 3. Photos illustrating magnetic targeting of microcapsules (a) before and (b) after magnetic targeting; (c) VSM of microcapsules; (d) low-field region of the VSM.

Acid and photo degradation of microcapsules

Herein, FITC-dextran is used as a model drug to investigate the drug release behavior of the microcapsules. During the degradation of the microcapsules, cotton-shaped suspended solids are observed from the group stimulated by pH. The strong non-covalent interactions such as host-guest interactions and Coulombic force of the cross-linked polymer chains turn them into a kind of hydrogel. The samples are collected at 0.25, 0.5, 1, 2, 4, 8, 21 and 25 h.

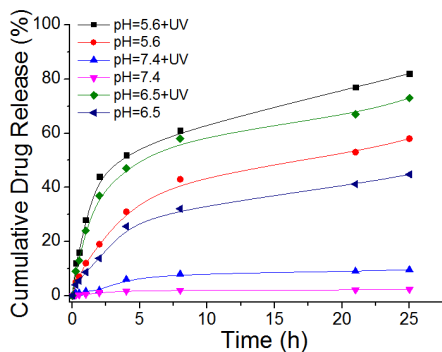


Figure 4. Cumulative drug release from the microcapsules under different conditions.

After ultrasonic treatment, the capsules are broken and the amount of FITC-dextran incorporated is measured. As shown in Fig. 4, drug release improves with pH and photo stimulation. In the neutral environment without UV light, only about 1.1% of the drug in the capsules is released in the first 2 hours, as a contrast, at a pH value of 5.6, about 19% of the drug is released. When UV light exposure is implemented in a neutral environment, about 2% of the drug is released in the first 2 hours but when UV light exposure is conducted at a low pH of 5.6, 44% of the drug is in the same time. Even at the pH of 6.5 with UV light exposure, 37% of drugs was released and 13.8% of drugs can be released without the UV light exposure. The results suggest that UV exposure and low pH can be used to control the release behavior. This “and” logic gate type drug release

behavior provides double insurance on drug release. In this system, a low pH plays a more important role than UV irradiation because once the C=N bonds in the β -CD-g-Dex are hydrolyzed, free β -cyclodextrin molecules can be released. Since the free β -cyclodextrin has a larger complex-dissociation constant with the host molecules, the β -cyclodextrin grafted to the polymer chain is replaced by the free β -cyclodextrin thus decreasing the interaction force between nearby layers. When both the inner and outer layers of the microcapsules are destroyed by UV and pH, the drug is released at a high rate. By using UV stimulation, the drug release rate is enhanced dramatically and this phenomenon indicates that the drug release characteristics can be controlled hierarchically. The same result can be found with the UV-vis spectrophotometer measurement as shown in Figure S1.

However, it should be noticed that the 365 nm ultraviolet light has a relative poor tissue penetration. Thus, the clinical application of the microcapsules has some limitations in deep tissue anti-cancer therapy. However, by using upconversion nanoparticles, the near-infrared light can be converted to UV light and thus fully solve the above problem and addresses a major concern for *in vivo* application of light-activated materials^{32,33}. However, long wavelength azo derivatives such as azotolane can provide a more flexible control for drug delivery systems³⁴.

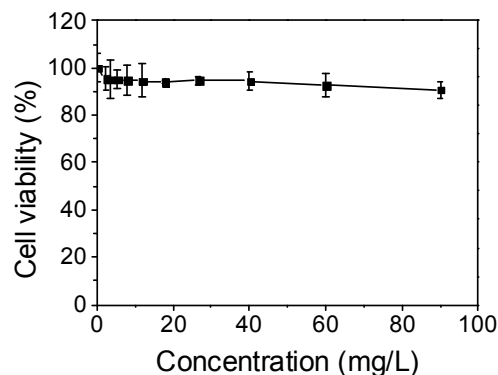


Figure 5. Cytotoxicity results based on HeLa cells by the MTT method with the microcapsules.

In vitro cytotoxicity

To evaluate the *in vitro* cytotoxicity of the microcapsules, the MTT assay is performed using the HeLa cell lines. After the cells are incubated with different concentrations of microcapsules for 24 h, Fig. 5 reveals good cytocompatibility during the incubation time with over 90% cell viability at a concentration of 90 mg/L. The results indicate that the microcapsules are non-toxic to the cells.

Co-Incubation of multi-stimulations microcapsules with cells at different pH values

Since the microcapsules can be stimulated by pH and UV light, four groups of experiments were carried to evaluate the ability of controlled release. HeLa cells are incubated with the microcapsules for 4 h at 37 °C. As shown in Figure 6, after incubation for 4 h, the HeLa cells stimulated by low pH and UV light show more green fluorescence than the other groups and less dextran accumulates in the HeLa cells after UV light exposure or at low pH than the control group.

Macromolecular drugs such as peptides, proteins, and polysaccharides are important anti-cancer drugs. Compared to other DDSs employing top-down methods to load drugs, for example, mesoporous silica nanoparticles and hydrogels, this bottom-up drug loading technique ensures that the macromolecular drugs can be encapsulated in LBL microcapsules more easily. Light exposure, pH, and magnetic field work together to release drugs controllably and precisely. Compare with low pH constituting passive targeting in the tumor micro-environment, UV light stimulation is active targeting for drug release. Meanwhile, the magnetic field provides a fast and exact way to locate the tumor position.

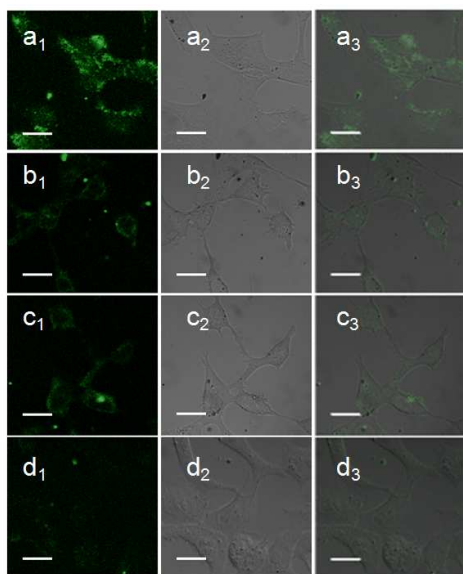


Figure 6. CLSM images of the microcapsules and HeLa cells co-incubated (a) with UV irradiation and low pH, (b) low pH, (c) UV irradiation, and (d) control group. (The scale bar was 20 μm) image 1: Green field; image 2: Bright field; image 3: overlapped field.

In vivo acute toxicity test

The microcapsules with doses of 100, 500 and 1000 mg/kg was subcutaneous injected into Balb/c mice ($n=5$) and all mice were survived at the 7th day. Thus, the result indicated that the subcutaneous LD_{50} of microcapsules was larger than 1000 mg/kg. Thus demonstrated the relative low toxicity of the microcapsules. After the experiment, mice were sacrificed. Tissue sections of heart, liver, kidney, lung and spleen were made and handled with H&E staining respectively (See Figure. S3). No obviously organ damage had been found and thus indicated that this microcapsules has low toxicity in vivo.

In vitro relaxivity measurement and in vivo pH response MRI

Magnetic resonance imaging is an important non-invasive cancer therapy. Fe_3O_4 nanoparticles have a superparamagnetic nature. The magnetic moment vectors relax rapidly when the external magnetic field is turned off and this property plays a key role in MRI negative contrast agents³⁵. In the MRI mechanism, a T2 contrast agent like Fe_3O_4 nanoparticles can decrease the signal intensity by shortening the transverse (spin-spin) relaxation time (T2) of water protons, resulting in negative effects in the interfered area³⁶. These negative contrast agents are determined by the transverse relaxivity (r_2) which represents the ability of the contrast agent to shorten the transverse

relaxation time (T2) of water protons. A clinical 9.4 T MRI instrument is used here to measure the transverse relaxation rates ($1/T_2$) and T2-weighted MRI.

As shown in Fig. 7, the small iron content group shows a white T2-weighted MR image and the MR signal declines with increasing concentration of Fe_3O_4 in the encapsulated microcapsules, confirming the ability of the microcapsules to enhance the transverse proton relaxation process. The r_2 relaxivity is calculated to be $92 \text{ mM}^{-1}\text{S}^{-1}$. However, when the pH of the solution is adjusted to 5.6, the r_2 relaxivity increases significantly by about 37% to $126 \text{ mM}^{-1}\text{S}^{-1}$. Since the pH of tumor tissues is normally lower than that of normal tissues, acid-responsive MRI provides better imaging for tumor tissues. The pH-responsive ability is mainly due to ionization of polyelectrolytes. Water protons that associated with bio-macromolecules (e.g., hydrogen bonded to protein and membrane surfaces) can restrict the mobility of water molecules, and, for this, have a shorter T2. Since the SPION has a carboxy-group-rich microenvironment, under acidic conditions, the carboxy groups can form hydrogen bonds with water to reduce the movement of water molecules. As a result, a shorter transverse relaxation time results.

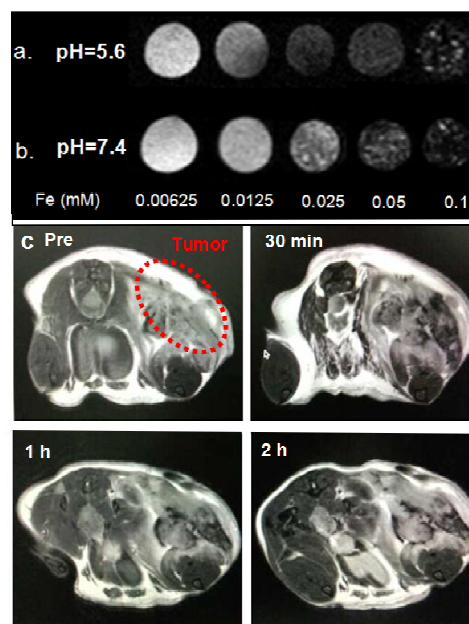


Figure 7. (a, b) T2-weighted MR images of the microcapsule solution with different iron concentrations at pH of 5.6 and 7.4; (c) T2-weighted MR images of mouse tumor before injection and at different time points after injection of microcapsules.

To evaluate the in vivo T2-weighted MR imaging ability, KM mice gave subcutaneous injection with Fe_3O_4 -encapsulated microcapsules and MR images were proceeded at different time points. Before injecting the microcapsules, the tumor manifests as a hyper-intense area in the T2-weighted MR images. After injection, significant darkening is observed and the resolution increases remarkably as well. Since tumors always have high signals in T1WI and T2WI, bright white is observed.

Generally, owing to the fast metabolic rate of tumors, metabolites such as lactate and carbonic acid accumulate in the tumors in the acidic micro-environment. In this respect, a low pH-response MRI contrast agent is very suitable for tumor diagnosis. The increase in r_2 of about 37% is obvious based on the in vitro experiments furnishing

evidence that the microcapsules provide better imaging ability in the acidic micro-environment.

In vivo magnetic targeting

The Prussian blue staining results was performed on mice for 48 h post-injection and the results were shown in Fig. 8. Many tumor cells were stained blue thus indicating the presence or accumulation of iron oxide. In comparison, in the magnetically targeted mouse, more blue dots are observed revealing that most of the microcapsules are concentrated in the tumor. The precise magnetic targeting ability provides a non-invasive method to concentrate the LBL microcapsules in the tumor.

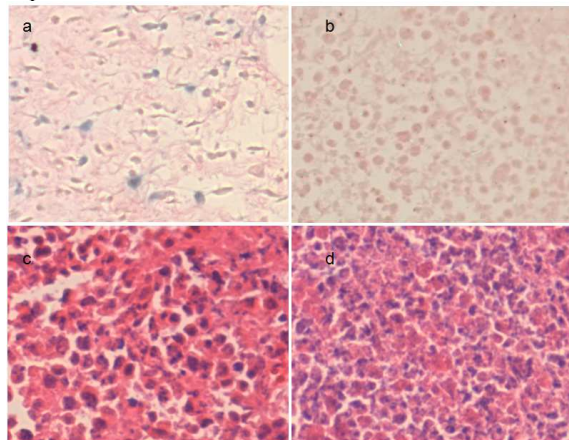


Figure 8. (a, b) Prussian blue stained images of tumor tissues (X 200) 48 h after injection of microcapsules with and without magnetic targeting; (c, d) Hematoxylin-eosin stained image of tumor tissues (X 200) 48 h after injection of microcapsules with and without magnetic targeting.

In vitro Stability Test

Since the microcapsules is based on self-assembly, so the stability in PBS, medium, and serum is investigated. As shown in Figure 9, after 12 h of co-incubation of microcapsules with PBS, DMEM, and serum, the morphology of the microcapsules is observed with CLSM. With the increase of serum concentration, a slight aggregation is observed. However, the aggregation was not serious. Thus, the result suggest that the microcapsules has a stability in medium or serum. Further more, the protein adsorption rate of microcapsules is calculated to be 0.2 mg/mg and the weak protein adsorption is mainly due to its negative zeta potential. The result indicate that the microcapsules is stable in physiological mediums.

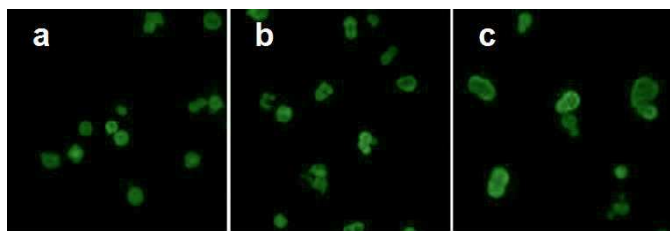


Figure 9. CLSM image of microcapsules after 12 h of co-incubation with (a) PBS; (b) DMEM and (c) FBS.

Conclusions

A multifunctional and intelligent micro-system responsive to light, pH, and magnetic field is developed using a simple LBL

method. The microcapsules are promising MRI contrast agents boasting an r_2 relaxivity of $126 \text{ mM}^{-1}\text{S}^{-1}$ in an acidic environment. This pH-responsive MRI contrast agent increases the r_2 relaxivity of tumor tissues and provides better contrast. Cell experiments confirm controlled drug release in *in vitro* and the magnetic targeting ability enables precise aggregation of microcapsules in *in vivo*. While it is a challenging to develop drug delivery systems that can transport macromolecular drugs to the right locations, the *in vitro* and *in vivo* results described here suggest that these microcapsules serve the dual role of effective pH response MRI contrast agents and drug delivery. The simple preparation procedures in conjunction with the cytocompatibility, superparamagnetism, and drug delivery ability of the materials bode well for the design of multimodal functional imaging probes for diagnosis of cancer.

Acknowledgements

This work was jointly supported by the National Natural Science Foundation of China (Grant no. 51273058), Ministry of Science and Technology of China (2011CB606202), City University of Hong Kong Strategic Research Grant (SRG) No. 7004188, and Hong Kong Research Grants Council (RGC) General Research Funds (GRF) No. CityU 112212.

References

- 1.D. Gupta, C. G. Lis. *Nutr. J.* 2010, 9, 1-16.
- 2.A. K. Gupta, M. Gupta. *Biomaterials* 2005, 26, 3995-4021.
- 3.S. Okada, S. Mizukami, T. Sakata, Y. Matsumura, Y. Yoshioka, K. Kikuchi. *Adv. Mater.* 2014, 26, 2989-2992.
- 4.H. E. Zhu, J. Tao, W. H. Wang, Y. J. Zhou, P. H. Li, Z. Li, et al. *Biomaterials* 2013; 34: 2296-2306.
- 5.Y. Zhong, F. Dai, H. Deng, M. Du, X. Zhang, Q. Liui, et al. *J. Mater. Chem. B.* 2014, 2, 2938 - 2946
- 6.J. T.-W. Wang, L. Cabana and M. Bourgoignon. *Adv. Func. Mater.* 2014, 24, 1880-1894.
- 7.J. Yu, C. Yang, J. Li, et al. *Adv. Mater.* 2014, 26, 4114-4120.
- 8.W. Li, L. Huang, X. Ying, Y. Jian, Y. Hong, F. Hu, et al. *Angew. Chem. Int. Ed.* 2015, 54, 3126 -3131
- 9.H. Luo, L. Lu, F. Yang, L. Wang, X. Q. Yang, Q. M. Luo, et al. *ACS Nano* 2014, 5, 4334-4347.
- 10.Z. W. Deng, Z. P. Zhen, X. X. Hua, Z. S. Xu, P. K. Chu. *Biomaterials* 2011, 31, 4976-4986.
- 11.M. R. Battig, Y. Huang, N. Chen, Y. Wang. *Biomaterials* 2014, 35, 8040-8048.
- 12.J. N. Liu, W. B. Bu, L. M. Pan, J. L. Shi. *Angew. Chem. Int. Ed.* 2013, 52, 4375-4379.
- 13.R. Duncan. *Nat. Rev. Cancer.* 2006, 6, 688-701.
- 14.K. Liang, G. K. Such, A. P. Johnston, Z. Y. Zhu, H. Ejima, et al. *Adv. Mater.* 2014, 26, 1901-1905.

ARTICLE

- 15.L. Qiu, T. Chen, I. Öçsoy, E. Yasun, C. Wu, et al. *Nano. Lett.* 2015, 15, 457-463
- 16.Z. Luo, Y. Hu, K. Y. Cai, X. W. Ding, Q. Zhang, M. H. Li. *Biomaterials* 2014, 35, 7951-7162.
- 17.Y. Chen, P. F. Xu, Z. Shu, M. Y. Wu, L. Z. Wang, S. J. Zhang, et al. *Adv. Funct. Mater.* 2014, 24, 4386-4396.
- 18.J. Tang, B. Kong, H. Wu, M. Xu, Y. C. Wang, Y. L. Wang, et al. *Adv. Mater.* 2013, 25, 6569-6574.
- 19.D. S. Ling, W. Park, S. J. Park, Y. Lu, K. S. Kim, M. J. Hackett, et al. *J. Am. Chem. Soc.* 2014, 136, 5647-5655.
- 20.S. I. Grivennikov, F. R. Greten, M. K. *Immunity. Cell* 2010, 140, 883-899.
- 21.G. P. Adams and L. M. Weiner. *Nat. Biotechnol.* 2005, 23, 2447-2457.
- 22.R. J. Youle and A. Strasser. *Nat. Rev. Mol. Cell. Bio.* 2008, 9, 47-59.
23. Q. Huang, T. Liu, C. Bao, Q. Lin, M. Ma and L. Zhu. *J. Mater. Chem. B*, 2014, 2, 3333-3339.
- 24.L. P. Lv, K. Landfester, D. Crespy. *Chem. Mater.* 2014, 26, 3351-3353.
- 25.A. Jana, K. T. Nguyen, X. Li, P. C. Zhu, N. S. Tan, H. Agren, et al. *ACS Nano* 2014, 6, 5939-5952.
- 26.A. Rodriguez-Pulido, A. I. Kondrachuk, D. K. Prusty, J. Gao, M. A. Loi and A. Herrmann. *Angew. Chem. Int. Ed.* 2013, 52, 1008-1012.
27. Y. Kang, K. Guo, B.-J. Li and S. Zhang. *Chem. Commun.*, 2014, 50, 11083-11092.
- 28.C. Li, G. F. Luo, H. Y. Wang, J. Zhang, Y. H. Gong, S. X. Cheng, et al. *J. Phys. Chem. C.* 2011, 115, 17651-11659.
- 29.M. G. Rodríguez, M. L. Tejada, J. Escalante, J. A. Guerrero-Álvarez, M. E. Nicho. *Mater. Chem. Phys.* 2010, 124, 389-394.
- 30.K. Yan, H. Li, P. H. Li, H. E. Zhu, J. Shen, C. F. Yi, S. L. Wu, et al. *Biomaterials* 2014, 35, 344-355.
- 31.D. Usov and G. B. Sukhorukov. *Langmuir* 2010, 26, 12575 - 84.
32. S. S. Lucky, N. M. Idris, Z. Li, K. Huang, K. C. Soo, and Y. Zhang. *ACS Nano* 2015, 9, 191-205.
33. Z. Jiang, M. Xu, F. Li, and Y. Yu. *J. Am. Chem. Soc.* 2013, 135, 16446-16453
34. F. Cheng, Y. Zhang, R. Yin, Y. Yu. *J. Mater. Chem.* 2010, 20, 4888-4896
- 35.Y. I. Park, H. M. Kim, J. H. Kim, K. C. Moon, B. Yoo, et al. *Adv. Mater.* 2012, 24, 5755-5761.
- 36.J. Lu, S. Ma, J. Sun, C. Xia, C. Liu, Z. Wang, et al. *Biomaterials* 2009, 30, 2919-2928.

Notes

a Hubei Collaborative Innovation Center for Advanced Organic Chemical Materials, Ministry of Education Key Laboratory for The Green Preparation and Application of Functional Materials, Hubei University, Wuhan, Hubei 430062, China

b Key Laboratory of Biomedical Polymers of Ministry of Education & Department of Chemistry, Wuhan University, Wuhan, Hubei 430072, China

c Department of Physics and Materials Science, City University of Hong Kong, Tat Chee Avenue, Kowloon, Hong Kong, China

* Corresponding author. Tel.: +86 27 88661729; fax: +86 27 88661729.

** Corresponding author. Tel.: +86 27 68754509; fax: +86 27 68754509.

*** Corresponding author. Tel.: +852 34427724; fax: +852 34420538.

E-mail addresses: zushunxu@hubu.edu.cn (Z. S. Xu), xz-zhang@whu.edu.cn (X.-Z. Zhang), paul.chu@cityu.edu.hk (P. K. Chu).

Graphic Abstract

Supramolecular Theranostic Capsules for pH-Sensitive Magnetic Resonance Imaging and Multi-responsive Drug Delivery

Di-Wei Zheng, Qi Lei, Si Chen, Wen-Xiu Qiu, Meng-Yi Liu, Xian Chen, Yu-Xue Ding, Peng-Hui Li, Quan-Yuan Zhang, Zu-Shun Xu, Xian-Zheng Zhang, Paul K. Chu

A novel Layer by layer (LBL) microcapsules with the function of macromolecular drug delivery and pH-stimulate MR Imaging capacity was designed and tested in both *vitro* and *vivo*.

